AKADÉMIAI KIADÓ

Pollack Periodica • An International Journal for Engineering and Information Sciences

18 (2023) 2, 17–22

DOI: 10.1556/606.2023.00799

ORIGINAL RESEARCH PAPER

Determination of influential springback parameters in U-bending test

Jemal Ebrahim Dessie* and Zsolt Lukacs

Faculty of Mechanical Engineering and Informatics, Institute of Materials Science and Technology, University of Miskolc, Miskolc-Egyetemváros, Hungary

Received: December 29, 2022 • Revised manuscript received: March 10, 2023 • Accepted: March 18, 2023
Published online: April 25, 2023

ABSTRACT

U-bending tests are the most common method to predict springback and are influenced by the process and geometrical variables in addition to material behaviour. It needs a numerical study at a high level with many variables to reduce try-out time and loop. In this study, the U-bending test of DC01 steel has been researched numerically and experimentally to govern the influential parameters. The numerical analysis was conducted using AutoForm-Sigma code. The die radius has an excessive influence on the change of flange angle than the punch radius, but the punch radius has the greatest influence on the variation of the sidewall angle. The coefficient of friction played a great impact on both flange and sidewall angle deviation and its influence grows stronger as the blank holding force increases.

KEYWORDS

AutoForm-Sigma code, coefficient of friction, DC01 steel, springback, U-bending

1. INTRODUCTION

Sheet metal bending is one of the most popular manufacturing techniques in which a homogenous material deforms around an axis that is orthogonal to the specimen's length direction and situated in the neutral plane [1]. Even though metal bending is a straightforward procedure, springback frequently interferes with it and is challenging to account for. The change in geometry of a stamped item must be compensated for, which raises the cost of manufacture [1]. After the tool is removed from the part, the component's dimensions change, and the stresses and strains in the material that underwent deformation change also [2]. The stamped portion is typically overbent to counteract this effect. One of the most crucial elements affecting contacting surface characteristics of the tool and sheet is the Blank Holding Force (BHF) [3]. Shape variation after sheet forming is mostly influenced by contact surface pressure and friction, and tool geometries [4–7].

By regulating a few process variables, Wang et al. [7] focused on analyzing springback that occurs during the stretch bending of sheet metal. It was found that a smaller die corner radius led to a smaller amount of sidewall springback due to the smaller required bending moment. Jiang et al. [1] studied the friction coefficient and blank holder force that affect the springback and have a reverse relationship. Angsuseranee et al. [8] explored springback and sidewall curl prediction in the U-bending process through the three-level tool geometry parameters and BHF at the constant coefficient of friction. The study confirmed that the springback decreases as increasing the BHF at a smaller punch radius. Tong et al. [9] numerically proposed a simplified method for obtaining material characteristics related to springback in addition to geometrical and process parameters. The investigation reached that the springback angle on the side wall is almost independent of radius of die. A detailed material model that accurately captures the Bauschinger effect is also necessary for accurate springback predictions. The springback was also impacted by the sheet thickness [10–12]. It is crucial to conduct a thorough optimization analysis of how changes to all examined parameters affect

*Corresponding author.
E-mail: metjemal@uni-miskolc.hu

the springback. Optimization of design variables is very critical and it needs a systematic approach [13].

In the ongoing research, the impact of frictional coefficient, BHF, and punch and die profile radius on springback prediction of the U-bending test for cold-rolled DC01 steel was investigated both numerically and experimentally. A commercial code AutoForm-Sigma was used for numerical investigation. AutoForm-Sigma enables a systematic improvement of the forming process. This is accomplished by varying the process and design parameters within a range that enables the development of safe processes [14]. High-level with multiple variables of Design Of Experiment (DOE) matrix has been simulated using Systematic Process Improvement (SPI). SPI increases transparency in the forming process by demonstrating, which design parameters influence the forming process and to what extent and it also helps to reduce the invested time and tryout loops, which is common in a conventional trial-and-error iterative approach to get the most efficient result. It is particularly true to estimate the coefficient of friction in a U-bending test because of difficult to calculate or measure in the physical experiment. As a result, it is possible to carry out experimental research at a low level of the design of experiment matrix to confirm some results of numerical simulation.

2. NUMERICAL SIMULATION OF U-BENDING TEST

U-bending of 250 × 20 × 0.45 mm rectangular cold rolled DC01 steel sheet was performed numerically using AutoForm commercial code. A uniaxial tensile test was used to determine the mechanical characteristic of the material as it is shown in Table 1.

Accurate springback prediction needs a material model which precisely describes the complex material behavior at loading-unloading conditions. In AutoForm commercial code, a novel approach has been developed and implemented to model the kinematic hardening behavior of the material [15, 16] as Eq. (1),

$$E_l = E_0(1 - \gamma(1 - e^{-\chi p})), \quad (1)$$

where E_l is the tangent modulus and which ordinarily falls off exponentially as comparable plastic strain p builds up; E_0 is the tangent modulus at zero plastic strain; χ is the saturation constant; γ is the Young's reduction factor formulated as Eq. (2),

$$\gamma = (E_0 - E_a)/\ E_0, \quad (2)$$

where E_a is the Young's modulus at infinite plastic strain.

Transient softening rate K is expressed by the summation of linear and non-linear reverse strain as Eq. (3) [17],

$$\varepsilon_r = \varepsilon_{rl} + \varepsilon_{rn} = \frac{\sigma_r}{E_1(p)} + K \times arctanh^2\left(\frac{\sigma_r}{2\sigma_h(p)}\right)^2, \quad (3)$$

where $\sigma_h(p)$ is the reverse plastic strain dependent isotropic stress; σ_r is the reverse stress curve; ε_r is the total reverse strain; ε_{rl} is the linear reverse strain; and ε_{rn} is the nonlinear reverse strain. This study considered a pre-defined kinematic hardening behavior in the material card of AuthoForm as it is shown in Table 2.

Multiple U-bending tests were numerically carried out automatically using SPI in a single simulation. Table 3 lists the design factors and their levels that were taken into consideration for the numerical analysis. The maximum BHF was decided because of the maximum compression force generated by the spring in the real physical experiment apparatus. Figure 1 shows the initial and the final geometrical setup before the removal of the punch.

3. EXPERIMENTAL PROCEDURES

Some samples of the U-bending test experiment were conducted in dry and lubrication conditions at a constant 5 mm tool radius profiles with the intention of validating the influence of friction and BHF on springback parameters, which was achieved in the numerical investigation. Figure 2 shows the experimental setup of U-bending die equipment,

Table 2. Kinematic hardening behavior of DC01

γ	χ	K
0.24	40	0.003

Table 3. Design variables and their level for the simulation

Parameters	Level
Radius of die profile, *Rd*, (mm)	3–10
Radius of punch profile, *Rp*, (mm)	3–10
BHF, (kN)	3–9
Coefficient of friction, μ	0.01–0.15

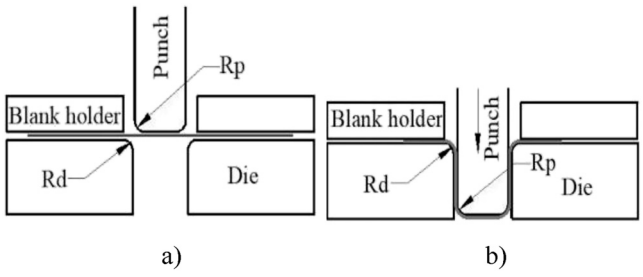

Fig. 1. Geometrical setup, a) before forming, b) after forming

Table 1. Mechanical and formability behavior of DC01

Elastic Modulus, E_0, (GPa)	Yield Stress, σ_0, (MPa)	Ultimate Tensile Strength (UTS), (MPa)	Total Elongation, A_g, (%)
206	192	322	24.5

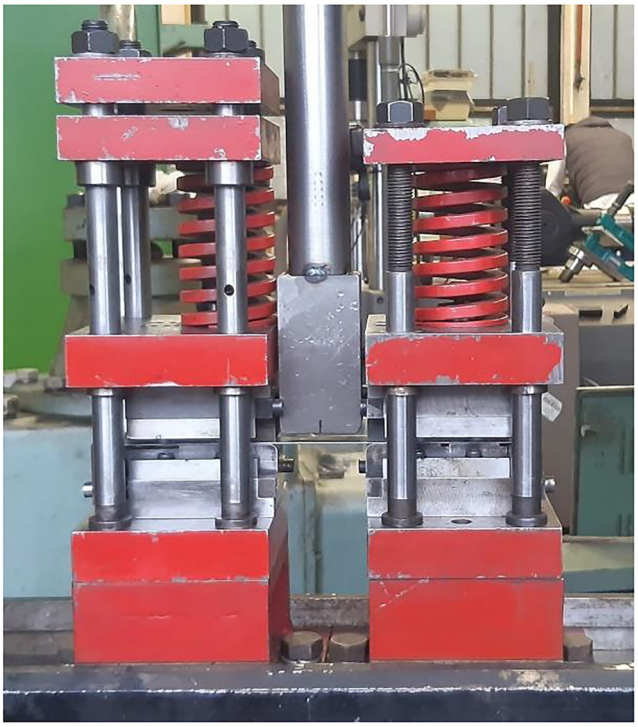

Fig. 2. U-bending die apparatus

which is installed on a 20 kN hydraulic press machine. Three-level spring-loaded BHF (at 3, 5, and 7 kN) was applied. The width of the punch was 40 mm and its half position matched the half position of the width of the sheet. The die and punch clearance on both sides was equal to double sheet thickness and the punch velocity was 5 mm s^{-1}.

4. RESULTS AND DISCUSSION

After removing of the tool, the 3D profiles in the simulation at $\mu = 0.05$ and $BHF = 3$ kN are shown in Fig. 3a and all 3D profiles in the physical experiments are provided in Fig. 3b. The amount of springback of each experiment and simulation was measured using NUMISHEET '93 benchmark standard [18] as it is shown in Fig. 4. The angle $\theta 1'$ and $\theta 2'$ were calculated using a simple relationship in Eq. (4),

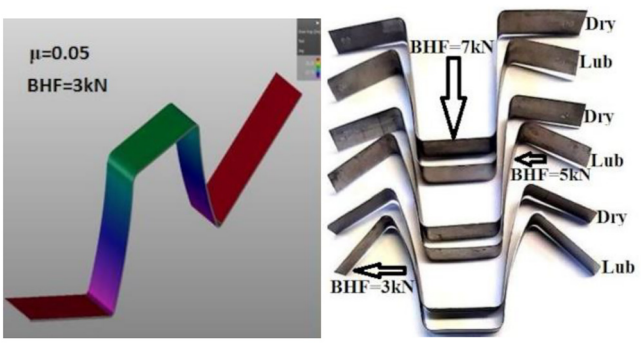

a) b)

Fig. 3. Springback profiles, a) simulation, b) experimental

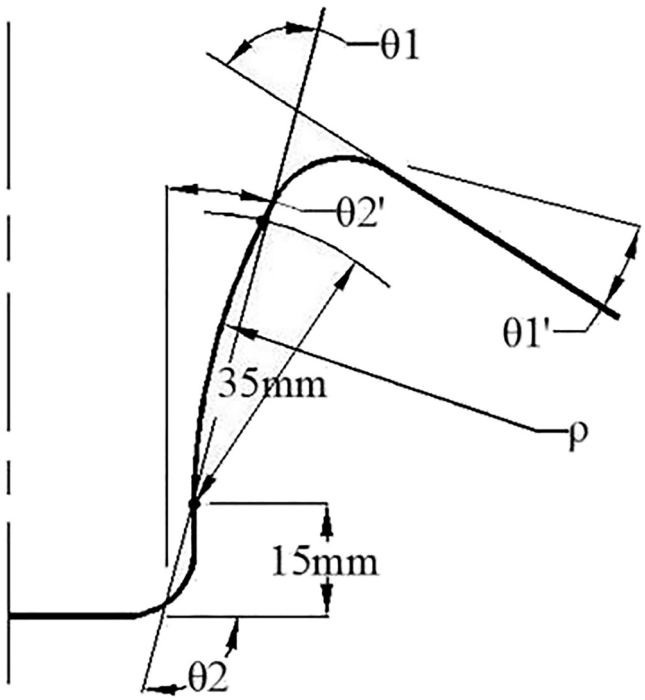

Fig. 4. Springback parameters in NUMISHEET '93 benchmark [18]

$$\theta 1' = 90 - \theta 1,\ \theta 2' = \theta 2 - 90. \tag{4}$$

The 2D picture of each sample in numerical and experimental results is exported to AutoCAD commercial drafting software to measure the springback parameters. Figure 5 shows the 2D profiles of all physical experiment samples after removing the tool. Numerical simulation at $Rd = 3$ and 4 mm and at $Rp = 10$ mm revealed distortion and excessive thinning. But in all other causes of process parameters, there were free from any distortion and excessive thinning.

4.1. Effect of die radius

In the numerical simulation, Fig. 6a and b show the effect of the Rd on the springback angle on the flange $\theta 1'$ and side

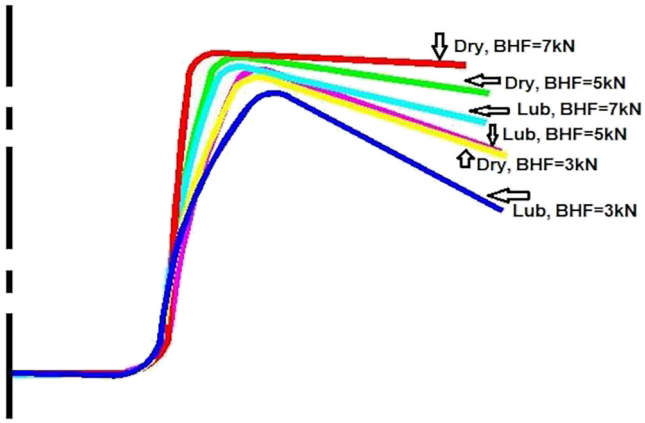

Fig. 5. 2D profiles of physical experiment samples after removal of the tool

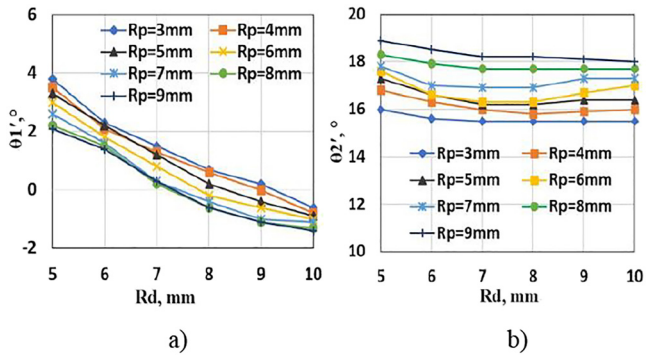

Fig. 6. Effect of the die radius in the numerical simulation, a) on the flange angle, b) on the sidewall angle

wall $\theta 2'$ at a different constant value of punch radius respectively. BHF was 3 kN and the coefficient of friction was 0.15 as constant in all causes. It can be seen in Fig. 6a that in the numerical simulation the springback angle $\theta 1'$ decrease with the increase of *Rd* because when *Rd* increases by a specific amount, the elastic strain created is no longer sufficient to cause any springback. It is interesting that the behavior of the angle $\theta 1'$ becomes negative when $Rd > 8$ mm at a constant value of $Rp > 6$ mm. This might be brought on by a further reduction in elastic strain close to the die corner. On the other hand, $\theta 2'$ has no significant effect on the *Rd* in the numerical simulation as it is shown in Fig. 6b. But, the value of constant *Rp* has a great impact on both $\theta 1'$ and $\theta 2'$, $\theta 1'$ decreases as increasing constant *Rp* but $\theta 2'$ increases with increasing constant *Rp*.

4.2. Effect of punch radius

Figures 7a and b show the effect of the *Rp* on the springback angle $\theta 1'$ and $\theta 2'$ respectively, in the numerical simulation. BHF was 3 kN and the coefficient of friction was 0.15 as constant in all causes. $\theta 1'$ is not affected by *Rp* but is highly affected by the constant value of *Rd* as it is shown in Fig. 7a. Angle $\theta 1'$ decreases as increasing of constant value of *Rd*. It is clearly shown in Fig. 7b that $\theta 2'$ is directly proportional to *Rp*. It increases as increasing *Rp* due to a reduction in the required contact pressure. The constant value of *Rd* has no discernible effect for $\theta 2'$.

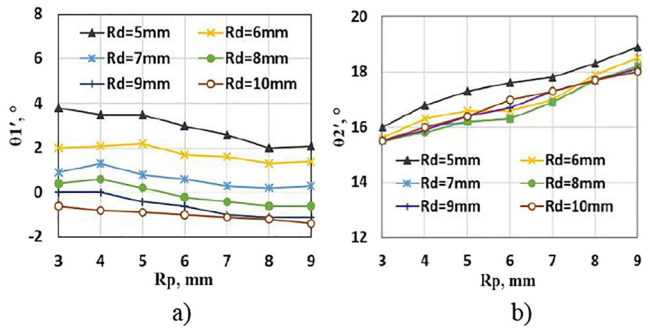

Fig. 7. Effect of the punch radius in the numerical simulation, a) on the flange angle, b) on the sidewall angle

The change in $\Delta\theta 1'$ and $\Delta\theta 2'$ at different level constant variables of *Rp* and *Rd* is shown in Fig. 8 using Eq. (5),

$$\Delta\theta 1' = \theta 1'\max - \theta 1'\min, \quad \Delta\theta 2' = \theta 2'\max - \theta 2'\min \tag{5}$$

In Fig. 7a, $\Delta\theta 1'$ and $\Delta\theta 2'$ was calculated from the maximum and minimum value found from variable *Rd* at a different constant level of *Rp*. But in Fig. 8b, $\Delta\theta 1'$ and $\Delta\theta 2'$ were calculated from variable *Rp* at a different constant level of *Rd*. The angle $\Delta\theta 1'$ is higher at every constant *Rp* but smaller at constant *Rd*. However, there was an overall decreasing tendency with the increase of constant *Rp* and fluctuating in the cause of constant *Rd* but the opposite relationship was found for $\Delta\theta 2'$. After all, *Rd* is the most influential parameter for $\theta 1'$ and *Rp* is the most influential for $\theta 2'$. To generalize, the result clearly shows the smaller value of $\theta 1'$ and $\theta 2'$ was found from $Rd = 10$ mm and $Rp = 3$ mm.

4.3. Effect of BHF and coefficient of friction

Controlling the BHF and coefficient of friction is one of the traditional methods to compensate springback. In order to study the relationship of BHF on springback, different BHF levels were selected from 3 to 9 kN. The advantage of finite element simulations is that easy to study the influences of coefficients of friction on the deformation process. In this study, the friction coefficient between tools and workpieces in the numerical analysis and it was varied from 0.01 to 0.15. The *Rd* and *Rp* were set at 5 mm as a constant value. Figure 9 shows the springback parameters as a function of

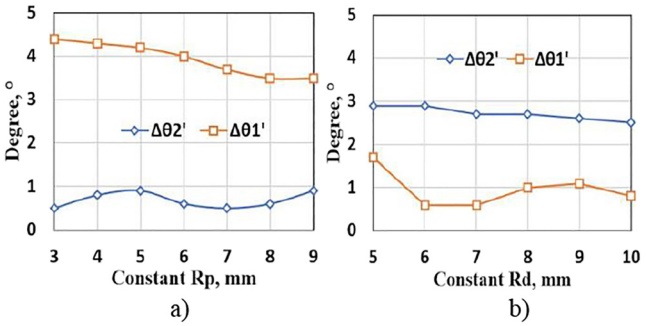

Fig. 8. Springback angle change, a) at constant *Rp* but variable *Rd*, b) at constant *Rd* but variable *Rp*

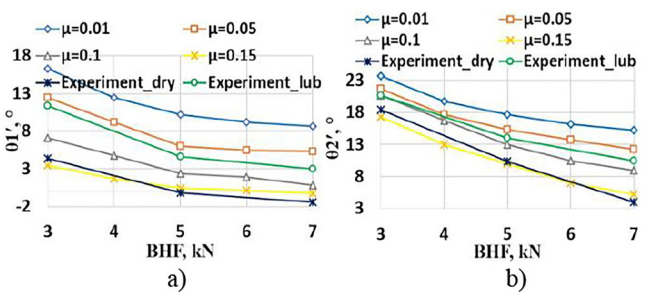

Fig. 9. Effect of BHF and coefficient of friction: a) on the flange angle; b) on the sidewall angle

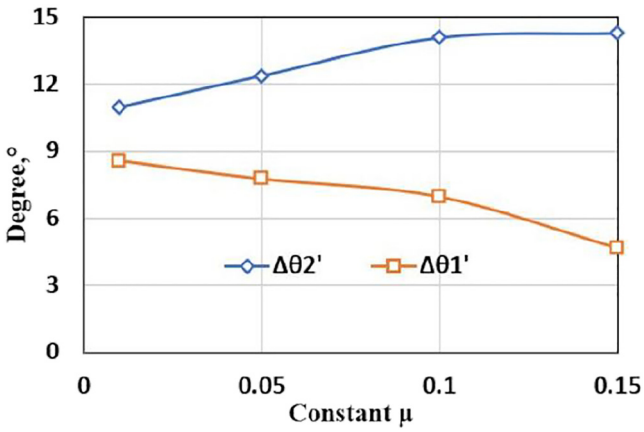

Fig. 10. Springback angle change at different level of constant coefficient of friction but variable BHF

BHF at different levels of constant coefficient of friction. The angle $\theta 1'$ and $\theta 2'$ have inverse relationships with BHF in all simulations. Springback decreases as increasing BHF because of a more uniform distribution of strains through the sheet thickness. It is clearly seen from Fig. 9 that springback parameters were almost closer amount in dry condition forming at $\mu = 0.15$ in the numerical simulation, on the other hand, the experimental test with lubrication condition forming was closer at between $\mu = 0.05$–0.10.

In Fig. 10, $\Delta\theta 1'$ and $\Delta\theta 2'$ was also calculated from the maximum and minimum value found from variable BHF at a different constant level of coefficient of friction. $\Delta\theta 2'$ is higher at every constant coefficient of friction and it increases as the increasing coefficient of friction but $\Delta\theta 1'$ has the opposite relationship. Therefore, the coefficient of friction is most influential for $\theta 2'$ than $\theta 1'$ and the influence becomes higher as increasing BHF.

5. CONCLUSION

The effects of process and geometrical parameters on springback phenomenon in the U-bending process have been explored numerically and experimentally. The numerical investigation with experimental verification is important and capable of predicting springback very accurately. A numerical investigation of the high-level with multiple variables design of the experiment matrix has been conducted using SPI and it is important to reduce the real physical design of the experimental study. Based on this study, the following remarks are drawn:

- The results produced by the analysis of the springback phenomenon using the finite element approach can be regarded as being sufficiently precise and valid;
- Die radius was the most influential geometrical parameter at the flange springback but punch radius is the most influential at the sidewall springback;
- The friction coefficient is one of the process variables that have a considerable impact on springback prediction, especially on the sidewall deviations. The influence becomes higher as increasing BHF.

REFERENCES

[1] H. J. Jiang and H. L. Dai, "A novel model to predict U-bending springback and time-dependent springback for a HSLA steel plate," *Int. J. Adv. Manuf. Technol.*, vol. 81, no. 5, pp. 1055–1066, 2015.

[2] R. Srinivasan, D. Vasudevan, and P. Padmanabhan, "Influence of friction parameters on springback and bend force in air bending of electrogalvanized steel sheet: an experimental study," *J. Braz. Soc. Mech. Sci. Eng.*, vol. 36, no. 2, pp. 371–776, 2014.

[3] L. A. de Carvalho and Z. Lukács, "Application of enhanced coulomb models and virtual tribology in a practical study," *Pollack Period.*, vol. 17, no. 3, pp. 19–23, 2022.

[4] A. Ghaei, D. E. Green, and A. Aryanpour, "Springback simulation of advanced high strength steels considering nonlinear elastic unloading–reloading behavior," *Mater. Des.*, vol. 88, pp. 461–470, 2015.

[5] H. L. Dai, H. J. Jiang, T. Dai, W. L. Xu, and A. H. Luo, "Investigation on the influence of damage to springback of U-shape HSLA steel plates," *J. Alloys Compd.*, vol. 708, pp. 575–586, 2017.

[6] H. Li, G. Sun, G. Li, Z. Gong, D. Liu, and Q. Li, "On twist springback in advanced high-strength steels," *Mater. Des.*, vol. 32, no. 6, pp. 3272–3279, 2011.

[7] A. Wang, K. Zhong, O. El Fakir, J. Liu, C. Sun, L. L. Wang, J. Lin, and T. A. Dean, "Springback analysis of AA5754 after hot stamping: experiments and FE modeling," *Int. J. Adv. Manuf. Technol.*, vol. 89, no. 5, pp. 1339–1352, 2017.

[8] N. Angsuseranee, G. Pluphrach, B. Watcharasresomroeng, and A. Songkroh, "Springback and sidewall curl prediction in U-bending process of AHSS through finite element method and artificial neural network approach," *Songklanakarin J. Sci. Technol.*, vol. 40, no. 3, pp. 534–539, 2018.

[9] V. C. Tong and D. T. Nguyen, "A study on spring-back in U-draw bending of DP350 high-strength steel sheets based on combined isotropic and kinematic hardening laws, "*Adv. Mech. Eng.*, vol. 10, no. 9, pages 1–13, 2018.

[10] B. Chongthairungruang, V. Uthaisangsuk, S. Suranuntchai, and S. Jirathearanat, "Springback prediction in sheet metal forming of high strength steels," *Mater. Des.*, vol. 50, pp. 253–266, 2013.

[11] X. Yang, C. Choi, N. K. Sever, and T. Altan, "Prediction of springback in air-bending of advanced high strength steel (DP780) considering Young′ s modulus variation and with a piecewise hardening function," *Int. J. Mech. Sci.*, vol. 105, pp. 266–272, 2016.

[12] A. J. Aday, "Analysis of springback behavior in steel and aluminum sheets using FEM," *Ann. de Chim. Sci. des Materiaux*, vol. 43, no. 2, pp. 95–98, 2019.

[13] K. Jármai and M. Petrik, "Optimization of asymmetric I-beams for minimum welding shrinkage," *Pollack Period.*, vol. 16, no. 3, pp. 39–44, 2021.

[14] AutoForm Engineering GmbH. [Online]. Available: https://www.autoform.com/. Accessed: Oct. 10, 2022.

[15] W. Kubli, A. Krasovskyy, and M. Sester, "Modeling of reverse loading effects including workhardening stagnation and early re-plastification," *Int. J. Mater. Forming*, vol. 1, no. 1, pp. 145–148, 2008.

[16] L. Wagner, M. Wallner, P. Larour, K. Steineder, and R. Schneider, "Reduction of Young's modulus for a wide range of steel sheet materials and its effect during springback simulation," *IOP Conf. Ser. Mater. Sci. Eng.*, vol. 1157, 2021, Paper no. 012031.

[17] M. Tisza and Z. Lukács, "Formability investigations of high-strength dual-phase steels," *Acta Metallurgica Sinica*, vol. 28, no. 12, pp. 1471–1481, 2015.

[18] NUMISHEET'93, *Proceedings of the 2nd International Conference Numerical Simulation of 3-D Sheet Metal Forming Processes; Verification of Simulation with Experiment*, Isehara, Japan, August 31–September 2, 1993.